Macromolecules

Article

How Knotting Regulates the Reversible Intrachain Reaction

Yu-Jane Sheng, Chien-Nan Wu, Pik-Yin Lai, and Heng-Kwong Tsao

More About This Article

Additional resources and features associated with this article are available within the HTML version:

- Supporting Information
- Links to the 1 articles that cite this article, as of the time of this article download
- Access to high resolution figures
- Links to articles and content related to this article
- Copyright permission to reproduce figures and/or text from this article

View the Full Text HTML

How Knotting Regulates the Reversible Intrachain Reaction

Yu-Jane Sheng,[*,†] **Chien-Nan Wu,**[†] **Pik-Yin Lai,**[‡] **and Heng-Kwong Tsao**[*,§]

Department of Chemical Engineering, National Taiwan University, Taipei, Taiwan, 106, R.O.C.; Department of Physics and Center for Complex Systems, National Central University, Jhongli City, Taiwan 320, R.O.C.; and Department of Chemical and Materials Engineering, National Central University, Jhongli City, Taiwan 320, R.O.C.

ABSTRACT: Knotted polymers have been found in biological systems, such as DNA knotting in phage capsids. Many biochemical reactions involve a close spatial contact between two reactive sites of a biopolymer and are often limited by the diffusive encounter rate of reacting groups. Therefore, the intrachain reaction is significantly regulated by topological constraints due to knotting. We investigated the reversible intrachain reaction of a knotted flexible polymer by Monte Carlo simulation and demonstrated that the intraknot association−dissociation crossover is mainly governed by both the essential crossing number and the topological similarity. Depending on the contour separation between reactive sites, the reaction may display qualitatively different behavior. The knotting (increment of the crossing number) favors the reaction with global contour separation but hinders that with local contour separation. In contrast to the latter case, the topological interactions of the former are clearly classified into different homologous groups, called Conway families. This result reveals that the biopolymer may utilize the relative contour separation of reactive sites and the knotting to control the intrachain reaction.

I. Introduction

Topological constraints are unavoidable in long polymers, and the static and dynamic properties[1,2] of the polymers are greatly influenced by these constraints. Knotted polymers depict a typical example of permanent entanglement. Various knotted polymers have been synthesized and found in chemistry and biological systems, such as DNA knotting in phage capsids.[3,4] Since topological properties of biopolymers, like DNA and protein, are essential for life, understanding the topological interactions of knotted polymers is of both fundamental and practical importance. The prime knot is characterized by various topological invariants, of which the values/forms remain unchanged regardless of how the knot is deformed. The conventional invariant of a knot $\mathscr{K}$ is the minimal number of crossings in any planar projection, denoted by $C_{\mathscr{K}}$. The number of essential crossings is a rather weak topological invariants because C can have a large degeneracy for large C. More sophisticated topological invariants such as Alexander and Jones polynomials are practically useful in knot identification for computer simulations.[5] However, it is not easy to derive any explicit topological properties or meanings from them.

The connection between topological properties and static and dynamic quantities of knot polymers, i.e., radius of gyration and nonequilibrium relaxation time, was studied. In general, the average crossing number,[6] radius of gyration,[7] and diffusivity[8] vary monotonically with C. Nonetheless, the extent of the data scattering grows with the crossing number because of the increasing degeneracy. On the other hand, the average writhe number[6] and untying relaxation time[9] must be classified

into different homologous groups according to the Conway notation or the Alexander polynomial. Within a group, these properties are clearly increased with C owing to the topological similarity. Those results indicate that the physical properties of a knotted polymer may be dominantly influenced by either the crossing number or the topological similarity (illustrated by the Conway notation[9]).

Many biochemical reactions involve a close spatial contact between two reactive sites of a biopolymer.[10] For example, site-specific recombination and initiation of transcription take place in a long DNA molecule. Such an intrachain collision is a random event caused by thermal fluctuations of the biopolymer conformation. Thus, the reaction is often limited by the diffusive encounter rate of reacting groups. The irreversible reaction of a linear polymer has been extensively studied.[11] Recently, the reversible reaction has also been explored both experimentally and theoretically.[12,13] Evidently, the topological interaction plays an important role in determining the diffusion-controlled intrachain reaction. In this work we investigate the influence of entanglement interactions on the reversible, intraknot reaction. The characteristics of topological constraints are manifested in terms of the knot type and the contour distance between the reactive sites.

II. Simulation Details and Two-State Model

We perform off-lattice Monte Carlo (MC) simulations to obtain the probability curves. There are three basic interactions in our model: the first is the hard-core excluded-volume interactions between monomers, which can be regarded as a knotted polymer having a finite cross-section thickness; the second is the prohibition of any segment crossing in the course of the kinetic process, and hence the knot is always the same type; the third is the binding interaction between the two chosen beads.

We consider various knotted ring polymers, which are made of N freely jointed, hard spheres with diameter σ

[†] National Taiwan University.

[‡] Department of Physics and Center for Complex Systems, National Central University.

[§] Department of Chemical and Materials Engineering, National Central University.

[*] Corresponding authors: E-mail hktsao@cc.ncu.edu.tw (H.-K.T.); yjsheng@ntu.edu.tw (Y.-J.S.).
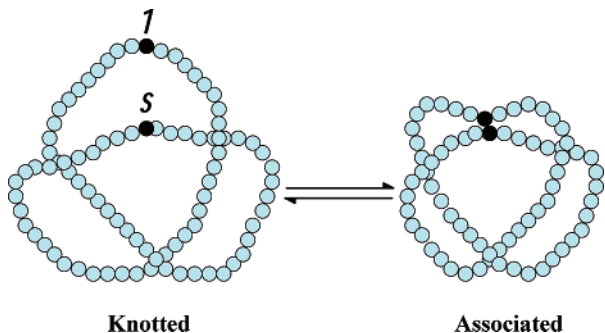
Figure 1. Fluctuation of the knotted polymer between knotted and associated states. The intraknot reaction is reversible.

tethered by slightly extensible bonds. We aim to explore knots with only topological constraint but without other extra interaction energies among monomers. Therefore, the interactions between the neighboring, bonded beads are through the infinite deep square-well potentials[12]

$$U_{i,i+1} = \infty \qquad r < \sigma$$
$$= 0 \qquad \sigma \leq r < \xi\sigma$$
$$= \infty \qquad r \geq \xi\sigma \qquad (1)$$

where $\xi = 1.2$. Bond crossing (phantom chain) can be prevented by such a choice. The reversible chemical reaction between two reactive groups located at beads "1" and "s" takes place when their center-to-center distance is less than $\lambda\sigma$ and the binding energy is $-\epsilon$. In other words, for this model knotted chain, the binding interaction between attractive beads 1 and s is represented by a standard square-well potential

$$U_{1,s} = \infty \qquad r < \sigma$$
$$= -\epsilon \qquad \sigma \leq r < \lambda\sigma$$
$$= 0 \qquad r \geq \lambda\sigma \qquad (2)$$

where $\lambda = 1.2$. Without the loss of generality, we assume the binding energy $\epsilon = 15$. It should be noted that the qualitative MC results will not be altered by the choice of the binding interaction.

As shown in Figure 1, the conformation is clearly identified as the associated state (a) when $\sigma \leq |\mathbf{r}_1 - \mathbf{r}_s| \leq 1.2\sigma$ and as the knotted state (k) otherwise. Note that the polymer in the associated state cannot be characterized by a knot $C_{\mathcal{K}}$. Similar to the melting curve depicting reversible looping of a linear polymer,[12,13] the variation of the fraction of the knotted state with temperature is displayed by the probability curve $P_k(T)$. The midpoint temperature T_m of the intraknot reaction is defined as the temperature where the probabilities of knotted and associated states are equal. Figure 2 illustrates the probability curves for different knot types with $N = 90$. As the temperature rises, the probable structure shifts from a stable associated state to a stable knotted one.

The systems simulated contain a single polymer knot with chain length N ranging from 42 to 128. The simulations are performed under the conditions of constant temperature and total number of beads. In the present study, the reduced temperature T^* is varied to obtain the melting curves, which are represented by $P_k = 1 - P_a$. The trial moves employed for chains of the equilibration and production process are bead displacement motions. They involve randomly picking a bead and displacing it to a new position in the vicinity of the
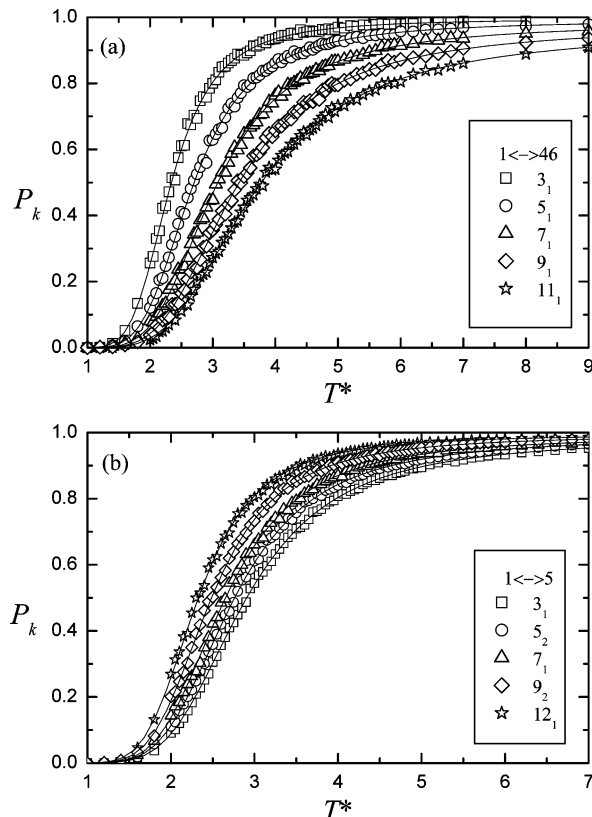

Figure 2. Variation of the probability of the knotted state with the scaled temperature $T^* = k_B T/\epsilon$ for various knot types with $N = 90$. The reactive sites are at (a) global contour separation (1 ↔ 46) and (b) local contour separation (1 ↔ 5).

old position. The distance away from the original position is chosen with a probability which satisfies the condition of equal sampling of all points in the spherical shell surrounding the initial position. The new configurations resulting from this move are accepted according to the standard Metropolis acceptance criterion. Runs for the same chain length at different temperatures are performed starting with the final configuration from a previous temperature and are equilibrated for 200 million steps. Measurements for static properties such as the probabilities of knotted or associated states are taken over a period of more than 10 million MCs per bead.

Despite many conformations associated with a knotted chain, they can be simply classified into the knotted and associated states for the intrachain reversible reaction. On the basis of the two-state scenario, one can obtain the probability curve for the association–dissociation crossover of a knotted polymer. In fact, the two-state model is successful in describing reversible loop formation of a hard-sphere chain.[12] The probability curve depicts the variation of the probability of the knotted state with temperature is given by

$$P_k(T) = \frac{1}{1 + e^{\epsilon(\beta - \beta_m)}} \qquad (3)$$

where β denotes the inverse temperature, $\beta = 1/k_B T$. The midpoint temperature is defined as

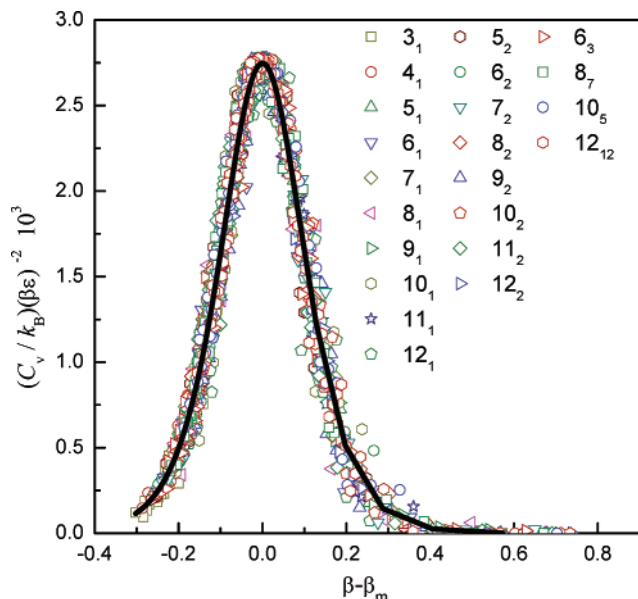$$\beta_m \epsilon = -\frac{S_a - S_k}{k_B} = \frac{\Delta S}{k_B} > 0 \qquad (4)$$

Figure 3. Universal heat capacity curve for various knot types. β_m denotes the midpoint temperature associated with a knot $C_{\mathcal{K}}$.

Figure 4. Variation of the midpoint temperature (or the entropy loss) with the essential crossing number at global contour separation with $N = 90$. Conway families are clearly shown.

where S_i represents the conformation entropy associated with the knotted hard-sphere chain at the state i. Note that $P_k = \frac{1}{2}$ at $\beta = \beta_m$. It can be seen clearly from eq 4 that $\beta_m\epsilon$ depicts the entropy loss associated with the knot-to-association transition. It can also be used to designate the probability of a particular configuration (beads 1 and s in close contact) for a pure hard-sphere chain without any reactive sites, $\exp(-\Delta S/k_B)$. In addition to the probability curve, thermodynamic quantities usually analyzed for the crossover of polymer conformations are the energy per monomer and the specific heat. Through the definition of heat capacity and by using eq 4, the C_v curve can be evaluated directly

$$\frac{C_v}{k_B} = \frac{P_k(1 - P_k)\epsilon^2}{(k_B T)^2} = (\beta\epsilon)^2 \frac{e^{\epsilon(\beta - \beta_m)}}{[1 + e^{\epsilon(\beta - \beta_m)}]^2} \quad (5)$$

It is also natural to identify the peak temperature of the heat capacity curve T_c as the characteristic temperature of knot-to-association transition.

III. Results and Discussion

The intraknot association−dissociation crossover are depicted by the probability curves for various knot types obtained from MC. As illustrated in Figure 2, the probability curves for different knot types can be well represented by eq 3. For a given chain length $N = 90$, β_m varies with the knot type $\mathcal{K}$ and the relative position of reactive sites $(1 \leftrightarrow s)$. As the essential crossing number is increased, the midpoint temperature increases in general for reactive site location $1 \leftrightarrow 46$ (global contour separation) but decreases for $1 \leftrightarrow 5$ (local contour separation). Note that $\beta_m(\mathcal{K}, s)$ determined by the fitting procedure is consistent with that read directly from the simulation data at $P_k = \frac{1}{2}$. In terms of the heat capacity curve, all data points of different $\mathcal{K}$ collapse into a single curve when we plot $(C_v/k_B)(\beta\epsilon)^{-2}$ against $(\beta - \beta_m)$. As shown in Figure 3, the heat capacity curve is well represented by eq 5. Those consequences indicate that the complicated topological effect in the
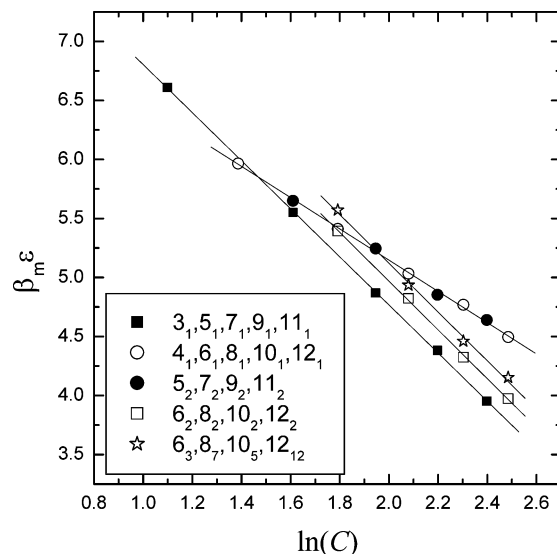
intraknot reaction is manifested through the midpoint temperature.

The knot-to-association crossover of a hard-sphere chain is the competition between binding energy gain and conformation entropy loss. The former is temperature-dependent while the latter is not. As a result, the knotted state is preferred at high temperatures and the associated state is dominant at low temperatures. The crossover temperature corresponds to the equal importance of binding energy and conformation entropy. Therefore, one has $\beta_m\epsilon$ corresponding to $\Delta S/k_B$, i.e., eq 4. It is not difficult to understand that the entropy difference (ΔS) of the knot-to-association transition depends strongly on the knot type. Different knots contain different topological constraints. Thus, eq 4 indicates that the influence of the topological constraint on the intraknot reversible reaction can be explored in terms of the crossover temperature. For a reactive pair $(1 \leftrightarrow s)$ under a constant temperature, the topological interactions associated with a knot $\mathcal{K}$ determine the conformation entropy loss and hence the midpoint temperature. Conversely, the characteristic of $\beta_m\epsilon$ manifests the topological nature associated with a knotted chain, as will be shown later.

The change of conformational entropy varies with the reactive pair, the knot type, and the chain length. Two limiting behaviors corresponding to global and local contour separation are observed for $\beta_m\epsilon(N, C_{\mathcal{K}}; s)$. The first limiting case is that the two reactive sites are at the largest separation in terms of the contour distance. That is, the second reactive site is half the total contour length away from the first one, i.e., $s = N/2 + 1$. As demonstrated in Figure 4, for a given chain length, although the inverse crossover temperature (β_m) in principle decreases with the crossing number (C), the variation is *irregular*. A similar phenomenon has been observed for the mean writhe number and untying relaxation time.[6,9] It should be noted that if various knot types are grouped into different homologous families (as guided by the lines in Figure 4), ordered variation with C emerges from such an irregular behavior. These groups include $(2, C)$ torus knots $(3_1, 5_1, 7_1, ...)$, even twist knots $(4_1, 6_1, 8_1, ...)$, and odd twist knots $(5_2, 7_2,$

9_2, ...), ..., etc. In fact, the prime knots of the same group possess the topological similarity, which is clearly displayed by the knot diagrams, also the Conway notation, or the Alexander polynomials.

A knot can be divided into n tangles, each one of which is a region in the projection plane surrounded by a circle such that the knot crosses the circle exactly four times.[14] For a oriented knot, the Conway notation $a_1 a_2...a_n$ means the diagram of a trivial two-string tangle obtained from a sequence of nonzero integers a_1, a_2, ..., a_n with a_i denoting $|a_i|$ crossings with sign $\epsilon_i = a_i/|a_i| = \pm 1$ ($i = 1, 2, ..., n$).[14] The minimum crossing number and the writhe of the knot $\mathscr{K}$ are then given by $C_{\mathscr{K}} = \sum_i |a_i|$ and $Wr_{\mathscr{K}} = \sum_i a_i$, respectively. The group with topological similarity is identified as the knots with the same tangles except the tangle j. As one goes from the knot $\mathscr{K}$ to its successor two new crossings are introduced in this particular tangle, $a_j + 2\epsilon_j$, with the rest of the tangles unchanged. The Conway notation of this family is simply $a_1 a_2...(a_j + 2p\epsilon_j)...a_n$ with p the integer. They are called the Conway families.[15] In addition to the aforementioned groups, other examples include (6_2, 8_2, 10_2, ...) and (6_3, 8_7, 10_5, ...). The crossing number and writhe number of the Conway family are simply $C_{\mathscr{K}}^* + 2p$ and $Wr_{\mathscr{K}}^* + 2p$, where $p = 0, 1, 2$, and $C_{\mathscr{K}}^*$ and $Wr_{\mathscr{K}}^*$ are associated with the leading member of the family. The topological similarity is also demonstrated in the Alexander polynomial. A general expression can be written down for the Conway family, such as $(C - 3) - (2C - 7)t + (C - 3)t^2$ for (7_4, 9_5, 11_{343}, ...).

In accordance with the topological similarity or the Conway families, the crossover temperature for the reactive pair ($1 \leftrightarrow N/2 + 1$) is increased with the crossing number. Figure 4 shows that $\beta_m \epsilon$ is linearly proportional to $\delta \ln C$ with $\delta = -2.06$ for (2, C) torus knots, (6_2, 8_2, 10_2, ...), and (6_3, 8_7, 10_5, ...) and $\delta = -1.32$ for even and odd twist knots, (4_1, 6_1, 8_1,...) and (5_2, 7_2, 9_2,...). The slope δ can be regarded as a first indicator of the knot class. The characteristic of the Conway family $\mathscr{C}_f$ can be further illustrated by the intercept constant $G(\mathscr{C}_f)$. Although $G(\mathscr{C}_f)$ are nearly the same for twist knots, significant differences are shown for the class $\delta = -2.06$. Also can be seen in Figure 4, the $\beta_m \epsilon$ of the $\{6_2\}$ family is lower than that of the $\{6_3\}$ family, which indicates the entropy loss of the $\{6_2\}$ family is smaller than that of the $\{6_3\}$ family. The result shows that the topological similarity dominates over the crossing number in determining the conformational entropy loss due to reactive pair ($1 \leftrightarrow N/2 + 1$) binding. Within a Conway family, the entropy loss declines logarithmically as the crossing number is increased. As C is increased for a given chain length, the radius of gyration declines and hence the conformational entropy is lowered. The association reduces the degree of freedom furthermore. However, the extent of reduction due to association is greater for smaller C.

The chain length also influences the conformational entropy. The loop formation of a linear polymer chain of length N costs the entropy loss, $\Delta S \propto k_B \ln N^\alpha$ with $\alpha = \nu(3 + g)$.[1,16] For a Gaussian chain, $\alpha = 1.5$ because of $\nu = 1/2$ and $g = 0$. However, for a self-avoiding polymer, one has $\alpha = 1.97$ for end-to-end contact with $\nu \approx 3/5$ and $g \approx 0.28$.[12] Here g denotes the correlation hole exponent which describes the short-distance spatial decay of the contact probability between two reactive sites due to the self-avoiding effects. Note that g is even larger for end-to-interior and inter-to-interior contacts.[16]
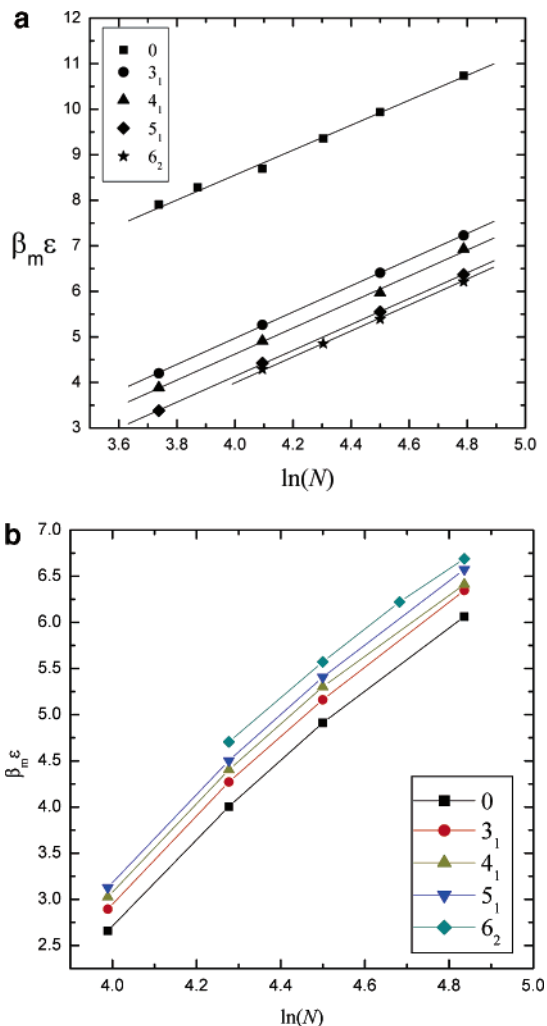
Figure 5. Variation of the midpoint temperature (or the entropy loss) with the chain length for various knot types: (a) at global contour separation ($1 \leftrightarrow N/2 + 1$); (b) at local contour separation ($1 \leftrightarrow 5$).

We anticipate that the same scaling law can be applied to the intraknot association. For reactive pair ($1 \leftrightarrow N/2 + 1$), Figure 5a shows the variation of $\beta_m \epsilon$ with the chain length for various knot types. Clearly, the scaling law still holds, however, with $\alpha = 2.85$. Since $\nu \approx 3/5$ for nonphantom polymer ring as for the excluded-volume linear chain,[17] one has $g = 1.75$ if $\alpha = \nu(3 + g)$ still holds. This result reveals that the topological effect enhances the self-avoiding influence on the correlation hole exponent. As a consequence, the entropy loss associated with the knot-to-association transition for the reactive pair ($1 \leftrightarrow (N + 2)/2$) is given by

$$T\Delta S = k_B T[\ln N^\alpha C^\delta + G(\mathscr{C}_f)] \tag{6}$$

This result clearly points out that the entropy loss due to association for a polymer ring is much greater than that due to looping in a linear chain. Similarly, Figure 5b plots $\beta_m \epsilon$ against $\ln N$ for local contour separation. To observe the scaling law correctly, one should consider the reactive pair ($1 \leftrightarrow N/18$) for different, long chain lengths. However, because of relatively shorter chains in the present study, we consider the reactive pair ($1 \leftrightarrow 5$) and obtain approximate linear lines, which give $\alpha \approx 3.56$. This outcome reveals that the entropy loss associated with local contour separation is greater than that
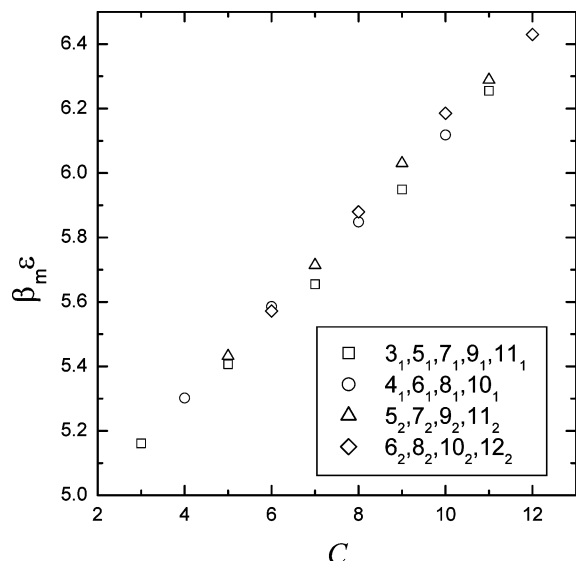
Figure 6. Variation of the midpoint temperature (or the entropy loss) with the essential crossing number at local contour separation $(1 \leftrightarrow 5)$ with $N = 90$. The essential crossing number effect dominates over the topological similarity.

of global contour separation for a given $\mathcal{K}$ with large enough N.

The behavior of $\beta_m \epsilon$ changes dramatically in the second limiting case: the contour distance (s) between the reactive sites is quite close, e.g., $(1 \leftrightarrow N/18)$. Contrast to the pair $(1 \leftrightarrow N/2 + 1)$, the inverse crossover temperature (β_m) in this case increases with increasing the crossing number. Moreover, the topological similarity plays a minor role, and the crossing number determines the general variation of $\beta_m \epsilon$, as shown in Figure 6. In other words, for the reactive pair $(1 \leftrightarrow N/18)$, the loss of conformational entropy due to association behaves the same way as the radius of gyration and the diffusivity. In general, the entropy loss due to association is linearly increased for a given chain length as C is increased. In the limit $1 \ll s \ll N/C$, the intraknot reaction takes place within a local region, and the region becomes smaller with increasing C. Because of the local nature of the reaction, the crossing number dominates over the global topological similarity.

Similar to the coil-to-loop crossover for a linear chain,[12] the knot-to-association crossover can be regarded as chemical equilibrium associated with a reversible reaction. The reactant and product are respectively the knotted and associated states, i.e., knot $\leftrightarrow$ association. At equilibrium, the principle of detailed balance is satisfied. The characteristics of the kinetics can be explored by examining the rate constants evaluated from MC simulations. The rate coefficients associated with jumping from the i to j states, $k_{i,j} = \tau_{i,j}^{-1}$, are assumed to follow the van't Hoff–Arrhenius law

$$k_{i,j} = k_{i,j}^0 \exp(-\beta F_{i,j}) \qquad (7)$$

where $F_{i,j}$ denotes the free energy barrier for jumping from the i to j states. The preexponential factor $k_{i,j}^0$ is independent of temperature and chain length. When the conformation of a knotted hard-sphere chain changes from the knotted state to the associated one, it is intuitive to expect that the free energy barrier corresponds to the entropy loss from a knot to an intraknot association, $\beta F_{k,a} = (S_k - S_a)/k_B$. As a consequence, $k_{k,a}$ does not depend on the temperature but varies with the
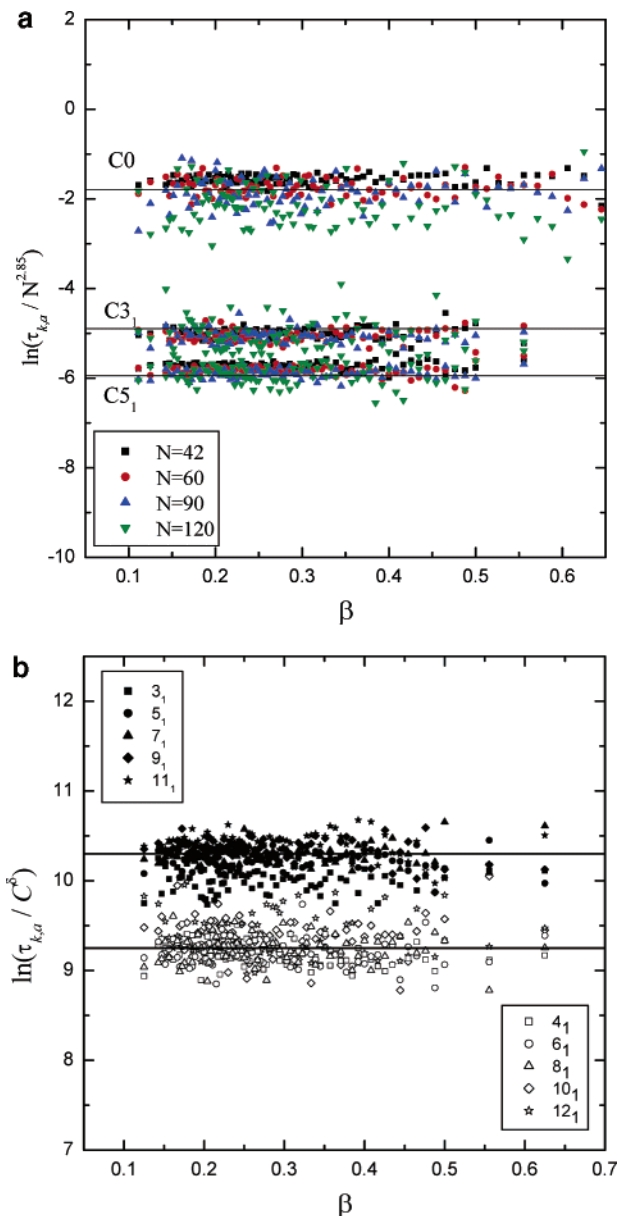

Figure 7. Variation of the association rate constants $k_{k,a}$ with the inverse temperature β for (a) different chain lengths of knot 0, 3_1, and 5_1 and for (b) two knot groups with $N = 90$.

chain length and knot type. For the reactive pair $(1 \leftrightarrow N/2 + 1)$, in accordance with eqs 6 and 7, one has

$$\ln\left(\frac{\tau_{k,a}}{N^\alpha}\right) = \ln C^\delta + G(\mathcal{C}_f) + \ln k_{k,a}^0 \qquad (8)$$

This result points out that $\Delta \ln(\tau_{k,a}/N^\alpha) = \Delta[\ln C^\delta + G(\mathcal{C}_f)]$. As shown in Figure 7a, all the rate constants of a specific knot type $\mathcal{K}$ computed from different chain lengths fall into a constant line with zero slope when $\ln(k_{k,a}^{-1}/N^\alpha)$ is plotted against β. As indicated in eq 8, the difference between the intercepts of 3_1 and 5_1 agrees with the difference of $\ln C^\delta$ for the torus knot group. Note that the rate constant $k_{k,a}$ for the trivial knot also follows eq 8 with $\delta = 0$ and a topological constant $G(\mathcal{C}_f)$ different from that of torus knot. Equation 8 can be further examined by plotting $\ln(\tau_{k,a}/C^\delta)$ against β at a given chain length $N = 90$. As shown in Figure 7b, all data points for torus knots and even twist knots are collapsed into two horizontal lines. The difference
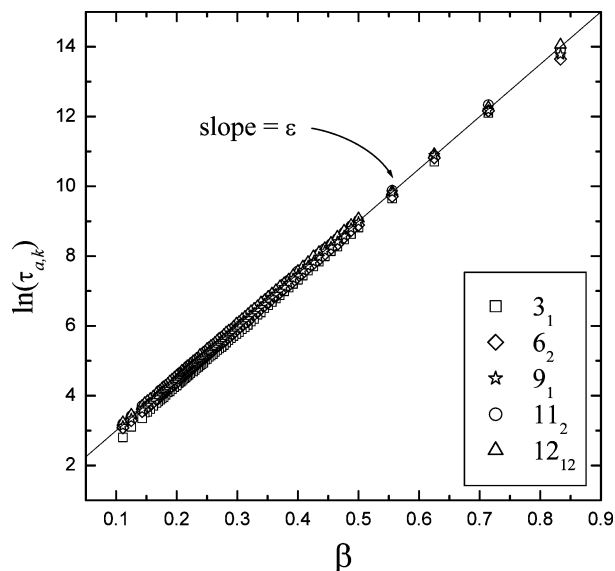
Figure 8. Variation of the dissociation rate constants $k_{a,k}$ with the inverse temperature β for various knot type with $N = 90$.
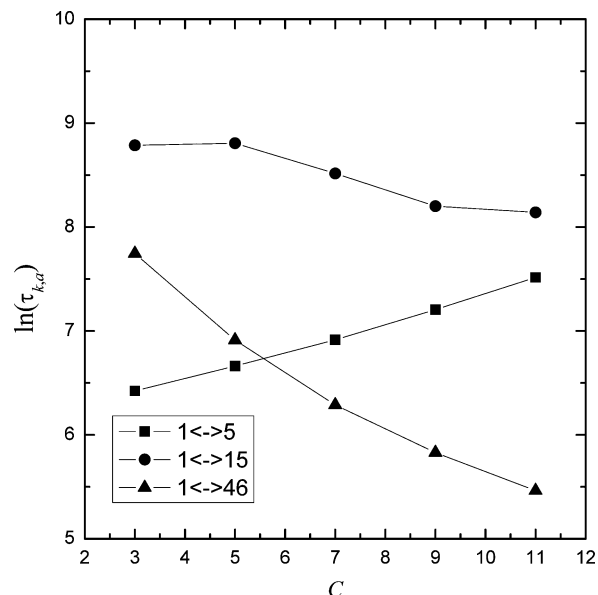

Figure 9. Plot of the association rate constant $k_{k,a}$ against the essential crossing number for different contour separation with $N = 90$.

between $G(\mathscr{C}_f)$ by kinetic analysis is 1.05, which is consistent with that obtained from the intercepts in Figure 4 by thermodynamic analysis, eq 6. This consequence confirms the validity of eq 6 for the conformation entropy change associated with knot-to-association crossover.

On the other hand, when the polymer conformation fluctuates from the associated state to the knot one, the free energy barrier, which has to be overcome, is simply the binding energy, $\beta F_{a,k} = \beta\epsilon$. Just like the linear chain, it must be independent of the chain length N. Moreover, it is irrelevant to the knot type $\mathscr{K}$. As illustrated in Figure 8, when $\ln(k_{a,k}{}^{-1})$ is plotted against β, all the rate coefficients calculated from different knot groups collapse into a single line with a slope of the binding energy ϵ. This outcome shows that the thermal fluctuation provides a probability of $\exp(-\beta\epsilon)$ to dissociate the associated conformation regardless of the knot type. The above analysis verifies the van't Hoff−Arrhenius characteristics of the rate constants $k_{i,j}$ for the knot−association equilibrium in terms of free energy barriers. The intraknot association−dissociation reaction is a result of the competition between binding energy gain (association) and conformational entropy loss (dissociation). When the binding energy ϵ is comparable to the thermal energy k_BT, the intraknot association is reversible. However, if $\beta\epsilon \rightarrow \infty$ for a finite chain length, the entropy gain $O(k_BT \ln N)$ is unable to compensate the binding energy loss at finite temperature. As a result, the formation of the associated state is favored and the reaction approaches irreversible.

From the thermodynamic viewpoint, the entropy loss associated with knot-to-association crossover is related to the contact probability between the two attractive beads and can be obtained through the midpoint temperature of the probability curve. Our MC results (Figures 4−6) show that the influence of the topological effect on the entropy change relies on the contour separation. In terms of reaction kinetics, Figure 9 also indicates that the effect of the topological interaction on the rate constant $\tau_{k,a}{}^{-1}$ depends on the reactive pair. For $N = 90$, the reaction rate is increased with C for (1 ↔ 46) but declines with C for (1 ↔ 5). The transition behavior is illustrated by the reactive pair (1 ↔ 15),

whose reaction rate is the slowest among the three cases. It is not surprising to see the consistent behavior between the midpoint temperature and the association rate constant because the free energy barrier is caused by the entropy loss. A simple, physical interpretation of such effects is given as follows: a knotted chain is more compact (which favors associated reaction) and still not too stiff (stretched) globally to kinetically discourage it. On the other hand, the local reaction is also disfavored since the chain is locally more stretched than the nonknotted one or since its part containing the reaction center is just winded around another one, which geometrically prevents an encounter of reactive entities. Recently, several works[18,19] show that the flat knots are strongly localized; i.e., the mean number of monomers in the knotted region does not depend on the total number of monomers. This knot localization might have decisive effect on the contact probabilities.

In summary, we have demonstrated that the physical properties of a knotted flexible polymer are mainly determined by both the minimum crossing number C and the topological similarity (Conway families). The association−dissociation crossover in a knotted chain can be well depicted by the two-state theory, i.e., the knotted and associated states. The midpoint temperature, equivalent to the entropy loss from the knotted to associated state, is obtained by Monte Carlo simulations. The lower midpoint temperature signifies the higher probability of association state (reaction). Depending on the contour separation between reactive sites, the intrachain reaction may display qualitatively different behavior. The knotting favors the reaction with global contour separation but hinders that with local contour separation. In contrast to the latter case, the topological interactions of the former are clearly classified into different homologous groups, called Conway families. Our results reveal that the biopolymer such as DNA may utilize the relative contour separation of reactive sites and the knotting to control the intrachain reaction.

References and Notes

(1) de Gennes, P. G. *Scaling Concepts in Polymer Physics*; Cornell University Press: Ithaca, NY, 1993.

(2) Schill, G. *Catenanes, Rotaxanes, and Knots*; Academic: New York, 1971.

(3) Wang, H.; Di Gate, R. J.; Seeman, N. C. *Proc. Natl. Acad. Sci. U.S.A.* **1996**, *93*, 9477.

(4) Arsuaga, J.; Vázquez, M.; Trigueros, S.; Sumners, De W.; Roca, J. *Proc. Natl. Acad. Sci. U.S.A.* **2002**, *99*, 5373.

(5) Deguchi, T.; Tsurusaki, K. *Phys. Lett. A* **1993**, *174*, 29.

(6) Huang, J.-Y.; Lai, P.-Y. *Phys. Rev. E* **2001**, *63*, 021506.

(7) Quake, S. R. *Phys. Rev. Lett.* **1994**, *73*, 3317. Grosberg, A. Y.; Feigel, A.; Rabin, Y. *Phys. Rev. E* **1996**, *54*, 6618.

(8) Sheng, Y.-J.; Tsao, H.-K. *J. Chem. Phys.* **2002**, *116*, 10523. Lai, P.-Y. *Phys. Rev. E* **2002**, *66*, 021805. Stasiak, A.; Katritch, V.; Bednar, J.; Michoud, D.; Dubochet, J. *Nature (London)* **1996**, *384*, 122.

(9) Lai, P.-Y.; Sheng, Y.-J.; Tsao, H.-K. *Phys. Rev. Lett.* **2001**, *87*, 175503. Sheng, Y.-J.; Lai, P.-Y.; Tsao, H.-K. *Phys. Rev. E* **1998**, *58*, R1222.

(10) Klenin, K. V.; Langowski, J. *Biophys. J.* **2001**, *81*, 1924.

(11) Wilemski, G.; Fixman, M. *J. Chem. Phys.* **1974**, *60*, 866. Szabo, A.; Schulten, K.; Schulten, Z. *J. Chem. Phys.* **1980**, *72*, 4350. Sokolov, I. M. *Phys. Rev. Lett.* **2003**, *90*, 080601.

(12) Sheng, Y.-J.; Chen, J. Z. Y.; Tsao, H.-K. *Macromolecules* **2002**, *35*, 9624. Tsao, H.-K.; Chen, J. Z. Y.; Sheng, Y.-J. *Macromolecules* **2003**, *36*, 5863.

(13) Goddard, N. L.; Bonnet, G.; Krichevsky, O.; Libchaber, A. *Phys. Rev. Lett.* **2000**, *85*, 2400. Sheng, Y.-J.; Lin, H.-J.; Chen, J. Z. Y.; Tsao, H.-K. *J. Chem. Phys.* **2003**, *118*, 8513.

(14) Kawauchi, A. *A Survey of Knot Theory*; Springer-Verlag: Tokyo, 1990. Adams, C. C. *The Knot Book*; W. H. Freeman and Co.: New York, 1994.

(15) Hoidn, P.; Kusner, R. B.; Stasiak, A. *New J. Phys.* **2002**, *4*, 20. Cerf, C.; Stasiak, A. *New J. Phys.* **2003**, *5*, 87.

(16) Sheng, Y.-J.; Hsu, P.-H.; Chen, J. Z. Y.; Tsao, H.-K. *Macromolecules* **2004**, *37*, 9257. des Cloizeaux, J.; Jannink, G. *Polymers in Solution: Their Modelling & Structure*; Oxford University Press: Oxford, 1990.

(17) Grosberg, A. Y. *Phys. Rev. Lett.* **2000**, *85*, 3858.

(18) Metzler, R.; Hanke, A.; Dommersnes, P. G.; Kantor, Y.; Kardar, M. *Phys. Rev. Lett.* **2002**, *88*, 18801. Metzler, R.; Hanke, A.; Dommersnes, P. G.; Kantor, Y.; Kardar, M. *Phys. Rev. E* **2002**, *65*, 061103.

(19) Orlandini, E.; Stella, A. E.; Vanderzande, C. *J. Stat. Phys.* **2004**, *115*, 681. Orlandini, E.; Stella, A. E.; Vanderzande, C. *Phys. Rev. E* **2003**, *68*, 031804.